SMARCB1 Deficiency in Tumors From the Peripheral Nervous System: A Link Between Schwannomas and Rhabdoid Tumors?

Daniela Rizzo, MD,† Paul Fréneaux, MD,‡ Hervé Brisse, MD, PhD,§ Camille Louvrier, MSc,‖ Delphine Lequin, BSc,¶ André Nicolas, BSc,‡ Dominique Ranchère, MD,# Virginie Verkarre, MD, PhD,** Anne Jouvet, MD,†† Christelle Dufour, MD,‡‡ Christine Edan, MD,§§ Jean-Louis Stéphan, MD, PhD,‖‖ Daniel Orbach, MD,† Sabine Sarnacki, MD, PhD,¶¶ Gaëlle Pierron, PhD,¶ Béatrice Parfait, PhD,‖ Michel Peuchmaur, MD, PhD,## Olivier Delattre, MD, PhD,¶*** and Franck Bourdeaut, MD, PhD†***

Background: Inactivation of *SMARCB1* tumor-suppressor gene was originally described as highly specific for rhabdoid tumors (RTs). Nevertheless, recent reports have illustrated that *SMARCB1* alterations also characterize other tumors; in particular, some familial schwannomatosis and epithelioid malignant peripheral nerve sheath tumors, both from peripheral nervous system (PNS) origin, lack BAF47 expression. To document the putative role of *SMARCB1* in PNS, we reviewed PNS tumors referred to our institution for a molecular analysis of *SMARCB1* because of histologic features compatible with RT.

Methods: Clinicopathologic, radiologic, and molecular characteristics were detailed for the 12 cases showing loss of expression and/or biallelic inactivation of *SMARCB1*. The status of the *NF2* gene, likely to synergize with *SMARCB1* in PNS tumors, was also analyzed.

Results: Patients' age ranged from 0 to 45 years (median age, 6.6 y). Neurological symptoms were observed in 7/12 cases with radiologic features evoking a neuroblastic tumor in 6 cases and a peripheral nerve tumor in 4 cases. The mean delay before diagnosis was 3 months. Histologic examination revealed rhabdoid features in 11/12 tumors. All tumors showed a complete loss of *SMARCB1* expression. Interestingly, adjacent nervous proliferation resembling neurofibromas were observed in 3 cases, suggesting a multistep transformation. Three tumors harbored a hemizygous deletion at the *NF2* locus, but all *NF2* sequences were normal.

Conclusions: We report the first series of PNS RT. In patients with aggressive PNS tumors, RT should be suspected, and anti-*SMARCB1* immunohistochemical analysis should be performed. *SMARCB1* inactivation, occasionally associated with *NF2* deletion, might have oncogenic effects in peripheral nerves.

Key Words: rhabdoid tumors, peripheral nervous system, *SMARCB1*, *NF2*

(*Am J Surg Pathol* 2012;36:964–972)

From the *Department of Pediatric Oncology, Catholic University, "A. Gemelli" Hospital, Rome; †Département d'Oncologie Pédiatrique; ‡Département de Pathologie; §Département d'Imagerie Médicale; ***INSERM U830, Institut Curie; ‖INSERM UMR745 & Service de Biochimie et Génétique Moléculaire, Hôpital Beaujon; ¶Institut Curie, Unite de Génétique somatique; **AP-HP Hopital Necker-Enfants Malades, Service de Pathologie; ‡‡Department of Pediatric Oncology, Institut Gustave Roussy; ¶¶Université Paris Descartes, AP-HP Hopital Necker-Enfants Malades, Service de Chirurgie infantile; ##Université Paris Diderot, Sorbonne Paris Cité, and Service de Pathologie, AP-HP, Hopital Robert Debré; #Centre Léon Bérard, Service de Pathologie; ††Service de neuroptahologie, Hospices Civils de Lyon, Lyon; §§Service d'hémato-oncologie pédiatrique, CHU Rennes, Rennes; and ‖‖Service d'hémato-oncologie pédiatrique, Université Saint-Etienne, Saint-Etienne, France.

Conflicts of Interest and Source of Funding: Supported by grants from the Associations Infosarcomes and Abigael. INSERM U830 is labelized by the Ligue Contre le Cancer. The authors have disclosed that they have no significant relationships with, or financial interest in, any commercial companies pertaining to this article.

Correspondence: Franck Bourdeaut, MD, PhD, INSERM U830 & Département d'oncologie pédiatrique, Institut Curie, Paris, France 75248 CEDEX05 (e-mail: franck.bourdeaut@curie.fr)

Supplemental Digital Content is available for this article. Direct URL citations appear in the printed text and are provided in the HTML and PDF versions of this article on the journal's Website, www.ajsp.com.

Rhabdoid tumors (RTs) are aggressive malignancies of early childhood, arising typically in the brain, kidney, and soft tissues. The main genetic characteristic of this malignancy is the biallelic inactivation of the *SMARCB1* gene, observed in approximately 90% of RTs.[6,45] *SMARCB1* acts as a tumor-suppressor gene, and inactivation of both copies in RTs leads to a total loss of its expression.[36] Hence, immunohistochemical analysis using an anti-BAF47 antibody is currently used as an adjunct to morphology for diagnosis.[7,27,28] Although loss of nuclear expression of *SMARCB1* was initially believed to be highly specific for RTs, a similar immunophenotype has recently been reported in other malignancies leading to potential nosological issues; however, epithelioid sarcomas,[24] renal

medullary carcinomas,[13] extraskeletal myxoid chondrosarcomas,[30] hepatoblastomas,[38] and cribriform neuroepithelial tumors[22] actually seem to be distinct from RT from a clinical and morphologic point of view, although sharing a loss of *SMARCB1* expression. Remarkably, among the *SMARCB1*-deficient tumors with nonrhabdoid diagnosis, Hornick and colleagues reported 12/24 cases of epithelioid MPNST (malignant peripheral nerve sheath tumor) harboring a loss of *SMARCB1* expression. This study was the first to report the link between peripheral nervous system (PNS) tumors and loss of expression of *SMARCB1* but without molecular analysis.[24]

Strikingly, recent studies also showed that *SMARCB1* germline mutations are the underlying cause of a subset of familial and sporadic schwannomatosis and rare forms of familial meningiomas.[9,11,20,25,26,35,37,39] Schwannomatosis is a genetic disorder characterized by the development of multiple schwannomas in the fourth to fifth decade of life. The occurrence of both RT and schwannomas within families with a unique *SMARCB1* germline mutation confirms that a common genetic disorder could be shared by these 2 types of tumors.[16,41] However, the molecular mechanisms elucidating how a germline *SMARCB1* mutation would lead to a benign late-onset PNS tumor or to an early aggressive RT remain elusive. Moreover, Eaton et al[16] recently described a familial case of RT initially diagnosed as MPNST, illustrating that *SMARCB1* germline mutation may predispose not only to benign schwannoma but also to malignant tumors of peripheral nerves with a rhabdoid phenotype.

Given the close vicinity of *SMARCB1* and *NF2* genes on chromosome 22q, recent studies assessed the concomitant deletion of both genes in schwannomas harboring 22q large deletions. Interestingly, these studies demonstrated that most *SMARCB1*-linked schwannomas show a multistep biallelic alteration of both *SMARCB1* and *NF2* through a documented "4-hit" mechanism.[14,20,21,26,35,39,44] Altogether, these data suggest not only that *SMARCB1* mutations play a critical role in the development of PNS tumors but also that a synergistic action of *SMARCB1* and *NF2* is a recurrent event.

Among the 150 RTs referred to our laboratory during the last 12 years, we identified 12 *SMARCB1*-deficient tumors potentially arising from the PNS. We therefore aimed at characterizing these tumors in detail from a clinical, radiologic, pathologic, and molecular point of view. We specifically investigated hypothetical similarities between these *SMARCB1*-deficient nervous tumors and other kinds of nervous tumors—that is, MPNST, neurofibromas, and schwannomas—through a detailed morphologic description and combined molecular analysis of *NF2* and *SMARCB1* genes.

MATERIALS AND METHODS

Inclusion Criteria

For the cohort study, the samples were selected from tumors referred from French pathology departments to our laboratory (Unité de Génétique Somatique, Institut Curie) because of pathologic features that were compatible with RT and therefore warranting a *SMARCB1* investigation according to the pathologist's discretion. From these approximately 150 samples, we selected tumors for which (i) a biallelic inactivation of *SMARCB1* and/or a total loss of SMARCB1 protein expression was actually registered, (ii) the anatomic origin was pointed out to be the PNS by the pathologist, or (iii) a differential diagnosis with MPNST, neurofibroma, or neurinoma was discussed in the pathologist's report. Finally, 12 BAF47-negative tumors matched these selection criteria and were considered for further description.

Clinical and Radiologic Characteristics

The clinical features that were assessed included: personal oncological history, sex and age at presentation, symptoms, location of the primary tumor, extension, first-line treatment modalities, and outcome. The time interval from onset of symptoms to the tumor diagnosis was recorded. To confirm the PNS as the origin of the tumors, radiologic data [magnetic resonance imaging (MRI) or computed tomography scan] were reviewed by a senior radiologist (H.B.).

Pathologic Analysis

Paraffin-embedded tissue was available for all patients. Representative hematoxylin and eosin-stained slides and initial immunostainings were initially reviewed by 3 experienced pediatric pathologists (P.F., M.P., and D.R.) according to the geographic provenance of the patients. M.P. and P.F. then reviewed all cases blindly and a consensus was reached. Immunohistochemical staining for vimentin, pancytokeratin, epithelial membrane antigen (EMA), glial fibrillary acidic protein, S100 protein, and tyrosine hydroxylase (TH) was recorded for all cases.

Immunohistochemistry (BAF47)

Immunohistochemical analysis was performed on formalin-fixed, paraffin-embedded tissue, and the activity of endogenous peroxidase was inhibited. The sections were placed in Dako Target Retrieval Solution High pH (Dako, Carpinteria, CA) and microwaved for antigen retrieval. The sections were incubated with the primary mouse monoclonal antibody BAF47 (BD Transduction Laboratories, San Diego, CA) for 1 h (1/100 dilution) at room temperature and washed with phosphate-buffered saline solution. After incubation with the Bond Polymer Refine Detection kit (Leica Biosystems Newcastle Ltd, UK) and staining with 3′-diaminobenzidine (Leica Biosystems Newcastle Ltd) as the chromogen, the slides were counterstained with Mayer hematoxylin, dehydrated, and cover-slipped.

Molecular Studies

DNA was extracted from frozen tumors according to classical procedures. All *SMARCB1* and *NF2* coding exons and splice site regions were sequenced using the Sanger method and the ABI automated fluorescent sequencer (primers and methods available on request).

TABLE 1. Summary of Clinical Features of the 12 Cases

Patient Number	Age at Diagnosis (mo)/Sex	Metastases	Localization	Radiologic Suspicion	Histologic First Diagnosis	Status	Follow-up (mo)
1	5/F	Y	Thoracic paravertebral sympathetic chain	NB	RT	DOD	3,5***
2	21/M	N	Brachial plexus L	NB	RT	NED	11
3	101/M	N	Thoracic paravertebral sympathetic chain	NB	RT	NED	49
4	0.6/M	Y	Cervical sympathetic chain	NB	RT	DOD	9
5	89/F	N	Cervical sympathetic chain	NB	RMS	DOD	11
6	18/M	N	Cervical sympathetic chain	NOS	RT/EC	NED	47
7	39/F	N	Sciatic nerve R	MPNST	MPNST	NED	49
8	35/F	N	Sciatic nerve R	ES	ES/MPNST	NED	133
9	18/M	N	Sciatic nerve L	NOS	RT	DOD	14
10	539/F	Y	Sciatic nerve L	NOS	Sarcoma	DOD	3
11	39/F	N	Pontocerebellar angle R	SCHW	NF	DOD	18
12	48/F	N	Pontocerebellar angle R	SCHW	MT	NED	30

DOD indicates died of disease; EC, embryonal carcinoma; ES, Ewing sarcoma; F, female; L, left; M, male; MT, mesenchymal tumor; N, no; NB, neuroblastoma; NED, no evidence of disease; NF, neurofibroma; NOS, not otherwise specified; R, right; RMS, rhabdomyosarcoma; SCHW, schwannoma; Y, yes.

Large-size deletions in the *SMARCB1* gene were searched for by the multiplex ligation-dependent probe amplification assay (MRC Holland, the Netherlands). Other genetic alterations were searched for by affymetrix SNP6.0 arrays.[42] Genomic DNA (500 ng) was processed according to manufacturer's recommendations. Data were analyzed with the Genotyping console software.

RESULTS

Clinical Features

Patients' features, treatment, and outcomes are summarized in Table 1. Mean age at diagnosis was 6.6 years (range, 0 to 45 y), and the diagnosis was made before 12 months in 2 patients. The tumors originated from the sciatic nerve in 4 patients (Figs. 1A, B), from the brachial plexus in 1 (Figs. 1C, D), from the thoracic paravertebral sympathetic chain in 2 (Figs. 2A, B), from the cervical sympathetic nerves in 3, and from the acoustic-facial nerves (pontocerebellar angle) in 2 (Figs. 3A, B).

Eight patients presented at diagnosis with neurological symptoms lasting for several months (up to 1 y; Supplementary Figure 1, Supplemental Digital Content 1 http://links.lww.com/PAS/A117). In these cases, the diagnosis of RT was not primarily suggested because of atypical location or slow-growing behavior (Table 1).

Radiologic Pattern

Radiologic review strongly suggested the PNS origin of the tumor in all patients. The mean diameter of the tumor was 5.8 cm (range, 1.5 to 9.5 cm). All tumors were well-circumscribed. A solid (9/12) or mixed (3/12) (solid and cystic) pattern was observed. Most tumors (10/12) demonstrated a heterogenous density on computed tomography or a heterogenous signal intensity on MRI, without any specific component (ie, no calcification or fat). Contrast enhancement was moderate to high in solid portions. Central necrosis was obvious in the largest tumors.

According to radiologic features, a neuroblastic tumor was the first diagnosis evoked in 5 cases, a benign neurofibroma or an acoustic schwannoma was suggested in 2 cases, and MPNST and peripheral primitive neuroectodermal tumor were the first diagnostic hypotheses in patients 7 and 8, respectively.

Pathology

Morphologic Features of the Tumor Cells

On the basis of morphologic features, the initial diagnosis was RT only in 5/12 tumors (initial diagnoses by local pathologists are reported in Table 1). The experts' review confirmed a highly cellular, malignant, solid neoplasm in all cases. Typical rhabdoid features, including (i) diffuse proliferation, (ii) round or polygonal cells, (iii) eccentric nuclei with prominent nucleoli and uncondensed chromatin, and (iv) eosinophilic cytoplasmic inclusions, were searched for. A completely rhabdoid phenotype was observed in 8 centrally reviewed cases. A partially rhabdoid phenotype (ie, when one of the previous items was not unambiguously found) was retrieved in 3 other tumors, and a consensus was achieved to conclude to a diagnosis of RT with incomplete features. In patient 8 in particular, the diagnosis of RT was finally retained because of the presence of scattered rhabdoid cells within undifferentiated cells with partially rhabdoid features.[31] One malignant, poorly differentiated tumor with nonrhabdoid features remained unclassifiable (patient 7, Supplementary Figure 2, Supplemental Digital Content 2 http://links.lww.com/PAS/A118).

Microscopic Relations Between Tumors and Peripheral Nerves

Pathologic analysis identified nervous structures in 6 cases: (i) sympathetic ganglion in 3 cases (patients 1, 3, and 5; Figs. 2C, D); in patients 3 and 5, the tumor was in close intimacy with a sympathetic ganglion but respected its architecture; (ii) large nerves, compatible with both

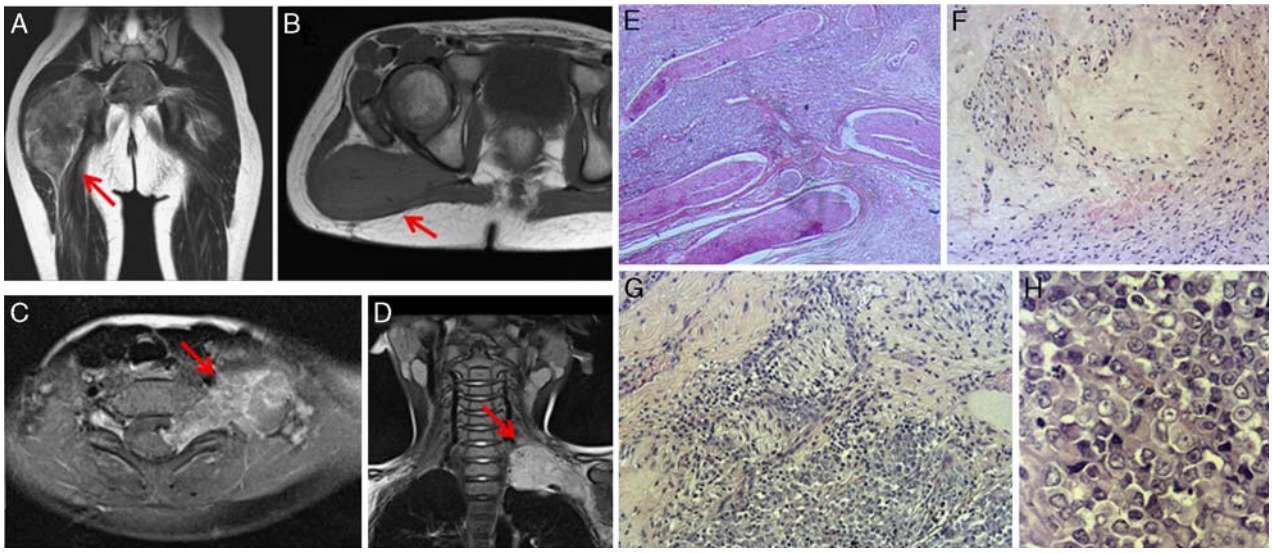

FIGURE 1. PNS tumors mimicking MPNST. MRI examination of patient 7: (A) coronal T2-WI and (B) axial T1-WI show a well-circumscribed lesion ($7 \times 4 \times 8$ cm) displacing gluteus maximus muscle arising from the sciatic nerve. The tumor (arrows) appears as a solid mass with isosignal on T1-WI as compared with muscles and heterogenous overall high signal intensity on T2-WI with nodular low signal intensities. MRI examination of patient 2: (C) postcontrast axial T1-WI and (D) coronal T2-WI show a solid dumbbell mass originating from the left C7-T1 foramen (spinal nerve and brachial plexus roots). The tumor (arrows) appears as a solid well-circumbscribed mass ($3 \times 6.5 \times 2$ cm) with heterogenous overall high signal intensity on T2-WI with nodular high signal intensities and heterogeneous enhancement after contrast media injection. Case 9: (E) coexistence in the same tumor of rhabdoid cell components and structurally hyperplasic and disorganized nervous structures characterized by different orientations of the fibers, both longitudinal and transverse, evoking the common findings of a benign nerve tumor that is neurofibroma-like. Case 2: (F) benign nervous component, showing obviously abnormal proliferation and organization of Schwann cells and fibrosis, resembling neurofibroma; (G) transition zone with intermixed rhabdoid component and benign nervous proliferation; (H) rhabdoid component. WI indicates weighted image.

normal nervous structures or benign nervous tumors, in 3 cases (patients 2, 9, and 11; Figs. 1E, F, 3C). The tumor in patient 11 showed an intimate juxtaposition and mixture of the different cell components, that is: Schwann cells displaying a normal morphology but abnormal proliferation that resembles schwannoma (Fig. 3C), fusiform cells showing marked atypia compatible with MPNST features (Fig. 3D), and finally typical rhabdoid cells (Fig. 3E). The tumors in patients 2 and 9, on the contrary, show a clear delimitation between the rhabdoid component and abnormal proliferative nervous structures (Figs. 1E, G). In these cases, the nervous structures were structurally disorganized, characterized by different orientations of fibers, both longitudinal and transverse, resembling the common findings of neurofibromas (Figs. 1E, F).

Immunohistochemical Features

To further relate the tumors to the rhabdoid phenotype, mesenchymal (desmin and vimentin) and epithelial markers (EMA and pancytokeratin) were recorded for all tumors (Table 2). Vimentin, EMA, and pancytokeratin stained positively in 8/12, 5/12, and 9/12 cases, respectively. Glial fibrillary acidic protein expression, assessed in the 2 intracranial (cerebellopontine angle) tumors, was obvious in both cases.

To bring more arguments in favor of a presumably nervous origin of the tumors, we also assessed the expression of S100 protein, a Schwann cell marker usually expressed in benign nervous tumors and in 80% of epithelioid MPNST.[15,19,43] A positive S100 staining was observed in 7/12 cases but exclusively in the Schwann cells.

As radiologic and morphologic findings suggested a sympathetic origin for some cases, we also investigated whether the TH, a protein normally present in catecholamines secreting neurons and in neuroblastic tumors, was expressed in the tumors in cases 1 to 6. Although an obvious expression was observed in some ganglion neurons in cases 1 and 5 (Fig. 2D), meanwhile confirming intimate relations of the tumors with the sympathetic system, no significant staining was evidenced in the tumor cells.

Finally, *SMARCB1* expression was carefully examined. Consistent with the inclusion criteria for this study, all tumors showed a clear loss of nuclear *SMARCB1* expression in rhabdoid cells. However, whenever observed in the same slides, the benign nervous component of the tumor retained a normal nuclear expression (Fig. 3F).

Genetic Features

SNP6.0 whole genome analyses could be performed on 9/12 tumors (Table 3, Fig. 4A). As expected in RTs, the mean number of chromosomal imbalances was no more than 2. Interstitial chromosome 22 deletion was

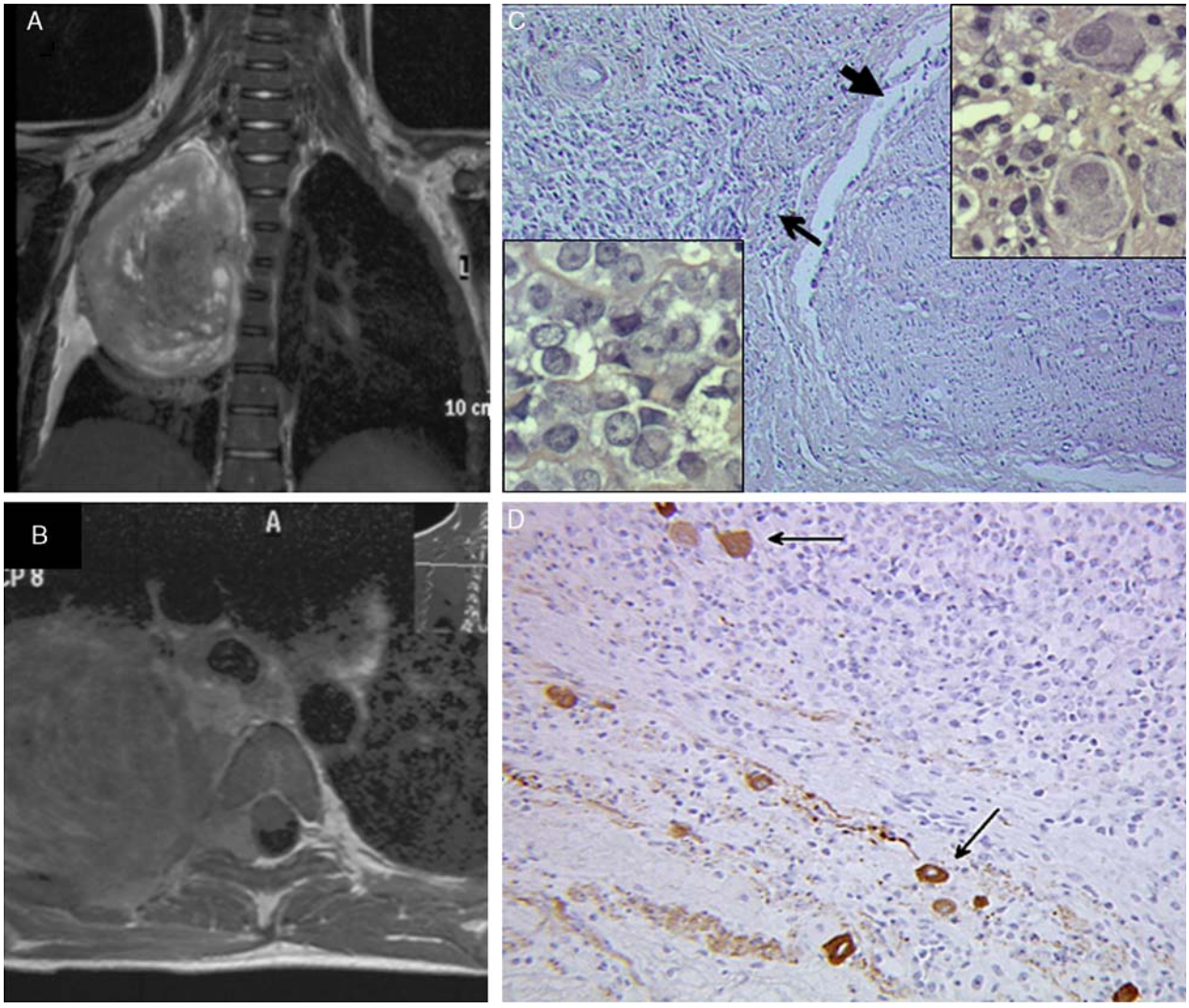

FIGURE 2. Posterior mediastinal RTs clinically mimicking neuroblastic tumors. MRI examination of patient 3: (A) coronal T2-weighted image and (B) postcontrast axial T1-weighted image show a large ($9.5 \times 7 \times 6$ cm) well-circumscribed solid thoracic dumbbell tumor arising from the paravertebral sympathetic chain, invading the posterior mediastinum, the pleural space, the T4-T5 foramen, and the epidural space. C, Coexistence of rhabdoid cells (thin arrow lower left) and sympathetic ganglion (thick arrow, upper right) (case 5). (D) Immunohistochemical staining for TH confined to ganglion neurons (case 1). Arrows show sympathetic ganglionnic neurons with TH expression.

observed in all cases. Noticeably, tumor 10, which arose in a 54-year-old adult, harbored a much higher number of chromosomal imbalances than the tumors arising in younger patients (Fig. 4A).

SMARCB1 status is summarized in Table 3. Biallelic inactivation was evidenced in 8/10 tumors tested. In 2 tumors, we could not discriminate between a genuine heterozygous deletion and a homozygous deletion in tumor cells diluted in a higher proportion of normal stromal cells. No frozen sample was available for the 2 remaining tumors.

NF2 direct sequencing found no mutation in the 7/12 analyzed tumors. Nevertheless, focusing on the *NF2* locus, SNP6 arrays allowed the detection of a hemizygous deletion of the *NF2* gene in 3 tumors (Fig. 4B).

Finally, as MPNSTs frequently show inactivation of *NF1*[19,43] and given that RTs have occasionally developed in an *NF1* context,[17] we also focused on the 17q11 region on SNP arrays. Neither deletion nor copy neutral loss of heterozygosity was evidenced at the *NF1* locus.

DISCUSSION

To the best of our knowledge, our work is the first to report alterations of *SMARCB1* expression in a series of pediatric PNS tumors. Given the recently enlarged spectrum of *SMARCB1* deficiency among malignant and benign tumors,[7,23] the first aim of our study was to assess whether these tumors were actual RTs. Our results confirmed that 11/12 of these tumors matched with RT

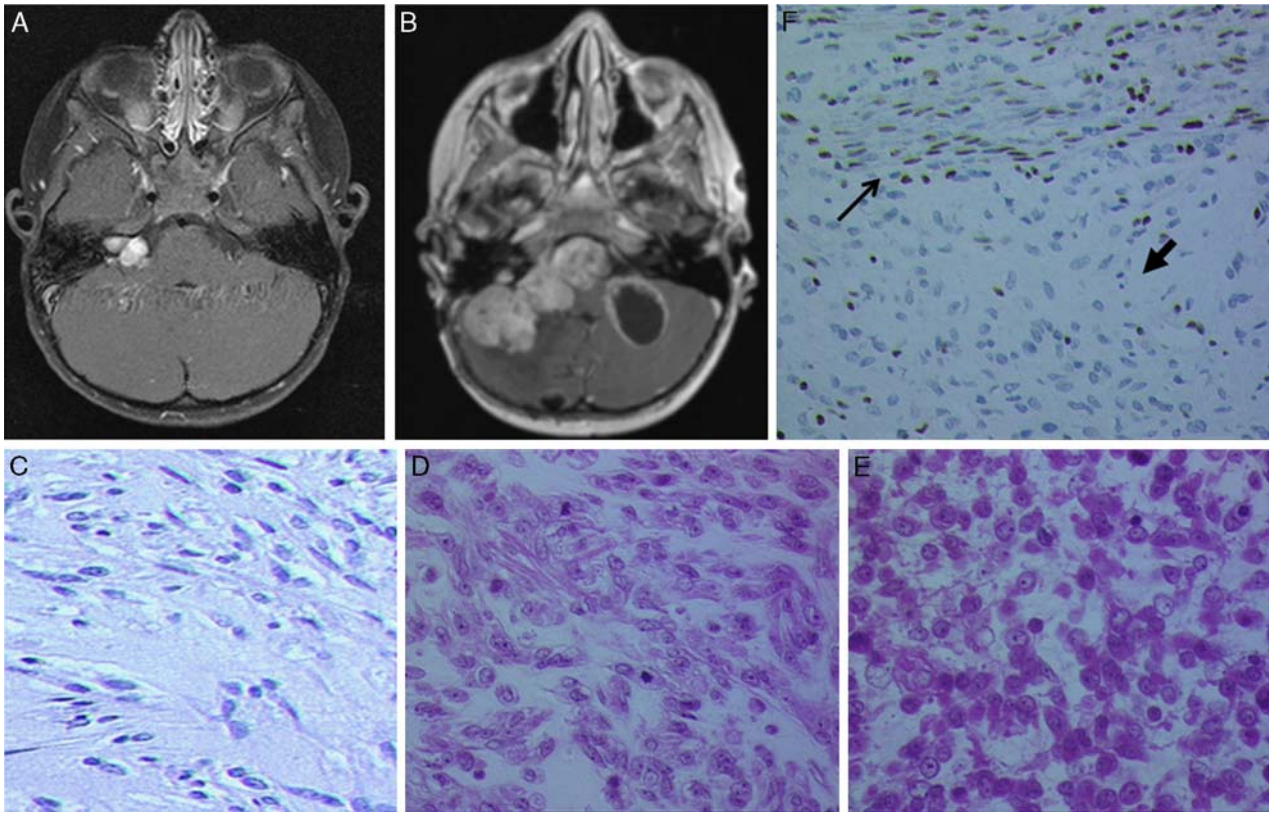

FIGURE 3. RTs arising from the cerebellopontine angle, mimicking acoustic schwannoma. MRI examination of patient 11: (A) postcontrast axial T1-WI show a small (1,5 × 1,2 × 1 cm) well-circumscribed enhancing mass originating from the right internal auditory canal or cerebellopontine angle. B, Postcontrast axial T1-WI: same tumor 4 months later, with major extension to cerebellopontine angle and cerebellum infiltration. The tumor demonstrates cystic (probably necrotic) components. C, First component of the tumor characterized by a proliferation of Schwann cells, organized in stacks of different orientations, evoking a neurinoma; (D) second area showing fusiform cells and marked atypia, strongly suggestive of MPNST; (E) third area with typical rhabdoid cells (case 11). F, *SMARCB1* is constitutively expressed in nonmalignant cells (Schwann cells and lymphocytes) (thick arrow), but completely absent in RT cells (thin arrow).

diagnosis either because of typical morphologic rhabdoid cells in all or part of the tumor or because of undifferentiated *SMARCB1*-deficient cells with a partially rhabdoid phenotype.[7] The positive staining with both mesenchymal and epithelial markers in all our tumors enforce their belonging to RTs, including case 7 that did not show significant rhabdoid features. On the contrary,

TABLE 2. Immunohistochemical Features of the 12 Cases

Case Number	Vimentin	EMA	CK	TH	GFAP	S100
1	+	ND	+	–	ND	Focal
2	+	ND	+	–	ND	Focal
3	ND	Focal	+	–	ND	Focal
4	+	–	+	–	ND	–
5	+	+	+	–	ND	Focal
6	–	Focal	+	–	ND	–
7	ND	–	+	ND	ND	–
8	+	ND	Focal	ND	ND	–
9	+	Focal	–	ND	ND	–
10	Focal	–	+	ND	ND	+
11	–	Focal	ND	ND	Focal	+
12	+	ND	ND	ND	Focal	Focal

CK indicates cytokeratin; GFAP, glial fibrillary acidic protein; ND, not done.

TABLE 3. Genetic Features of the 12 Cases

Case Number	*SMARCB1*	*NF2*	Chromosomes Imbalances
1	hD	wt	ND
2	HD	wt	del 9q, del 22q
3	ND	wt	del 13q, del 8p, del 22q
4	HD [1-3]	wt	del 22q
5	HD	ND	del 22q
6	HD	hD	del 22q
7	HD [1-5]	hD	del 10q, del 22q
8	HD	ND	ND
9	HD	wt	del 22q
10	hD	hD	gain 2, gain 8p, gain 21 del 9p, del 10q, del 18p, del 22q
11	HD	wt	gain 8p, del 22q
12	ND	ND	ND

del indicates deletion; [1-5], exons 1 to 5; hD, hemizygous deletion; HD, homozygous deletion; ND, not done; wt, wild type.

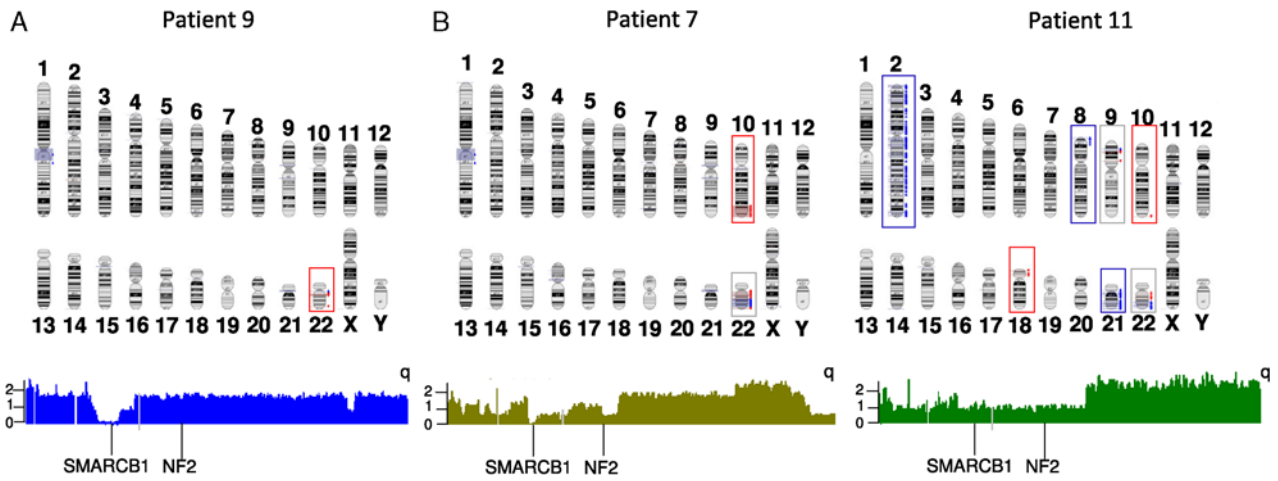

FIGURE 4. Chromosomal imbalances evidenced by affymetrix SNP6.0 arrays. A, Chromosomes in squares show imbalances; blue square and arrows refer to gains, and red square and arrows refer to deletions. Gray squares indicate that both gains and losses are observed within the same chromosome. B, Focus on chromosome 22. Short arm is on the left, long arm (q) on the right. The estimated number of copies is indicated for each probe, matching that of chromosome 22 in the left scale: "0" refers to homozygous deletion, "1" to hemizygous deletion, and "2" to a normal status. Lines above the "2" level indicate gains of chromosomal regions. *SMARCB1* and *NF2* loci are indicated for each tumor.

lack of TH expression in sympathetic nervous system tumors excludes a mature sympathetic neuron origin. Negative or focal staining of S100 in 10 tumors distinguished their immunophenotype from that of common benign Schwann cell–derived tumors and from epithelioid MPNSTs, which are known to retain the S100 expression.

A second aim of the study was to ascertain the nervous system origin of those tumors. Radiologic review confirmed the PNS tumor origin in all cases. Moreover, we unexpectedly observed some features compatible with benign nervous proliferation within or near the rhabdoid components. Given the recent works showing the links between *SMARCB1* germline mutations, acquired *NF2* somatic inactivation in Schwann cells, and development of schwannomas,[9,11,20,25,26,35,37,39] a potential genetic relationship between common PNS tumors—that is, neurofibromas, schwannomas, and MPNST—and our cases actually required further investigation. Although *NF2* constituted an attractive candidate gene, we found only 3 hemizygous deletions and no mutation. These results should be put in light of previous studies showing frequent 22q11 deletions in MPNST, without recurrent *NF2* mutations being reported so far. However, because of restricted biological samples, *NF2* could be sequenced in only 7/12 tumors, and a more exhaustive analysis would be required; in particular, the 2 tumors arising in the acoustic nerve, the most likely to be related to *NF2* mutations, could not be analyzed.

At least 3 hypotheses can be raised to explain the coexistence of benign nervous structures and rhabdoid proliferations:

1. Abnormal proliferation of normal Schwann cells as a reaction to the presence of neoplastic components nearby, as it is proposed for Schwann cells in neuroblastic tumors.[2]
2. A multistep malignant transformation of a preexistent benign nervous lesion. In this hypothesis, the rhabdoid features would be secondarily acquired from a primary nonrhabdoid proliferation by the biallelic inactivation of *SMARCB1*, as described in other glial tumors[1,12] and as suggested by Carter et al[11] in PNS. This hypothesis of a multistep tumoral evolution might account for the long delay between first neurological symptoms and diagnosis observed in some patients. In particular, patient 11 had a tumor genuinely resembling an acoustic schwannoma in MRI with some histologic features strongly suggestive of that diagnosis, whereas features were typical for RT both on MRI and histology a few months later. Similarly, patient 5 (Fig. 4) had a 12-month-lasting clinical history, a delay strikingly unexpected for RTs, which are usually characterized by rapid and aggressive symptoms.
3. The concomitant proliferation of different lineages arising from a common progenitor, as we previously suggested in some neuroblastic tumors with abundant Schwann cell proliferation.[8] This hypothesis is plausible, given that such composite features are described in other pediatric malignancies, such as Triton tumors or ectomesenchymomas.[3,29,32] In that respect, our observation would open new insights in a presumable neural crest cell origin of some RTs.

Finally, our study brings some clinical information with more practical aspects. Indeed, occurrence of RTs in unusual locations has been reported, including mediastinum, liver, neck, shoulder, and retroperitoneum.[5,10,18,33,34] In a large retrospective series of atypical nervous tumors, Strom et al[40] reported 1 case of PNS RT, and 2 other cases involving third and fifth cranial nerves have been previously described.[4,46] Our observations suggest that a misdiagnosis

with other entities, such as neuroblastoma and schwannoma-at least from a clinicoradiologic point of view-and epithelioid MPNST on a pathologic aspect, should be anticipated. Therefore, we recommend that anti-BAF47 immunohistochemistry should be widely performed in aggressive tumors involving peripheral nerves, either in cases highly suggestive of RT or in tumors of much less typical clinical and pathologic diagnoses.

ACKNOWLEDGMENTS

The authors thank all the pathologists who kindly provided them the tumor samples: Dr Pascale Marcorelle, Dr Elizabeth Cassagnau, Dr Marc Polivska, Prof. Aurore Coulomb, Dr Alix Clemenson, Dr Stephan Saikali, and Dr Sébastien Lepreux. The authors thank Prof. Alain Durandeau and physicians from the Societe Française des Cancers de l'Enfant (SFCE) for providing the clinical data. The authors thank Dr David Gentien from the Departement de Transfert, Institut Curie. The authors finally thank the molecular genetic platform of INCA and the Associations Infosarcomes and Abigael.

REFERENCES

1. Allen JC, Judkins AR, Rosenblum MK, et al. Atypical teratoid/rhabdoid tumor evolving from an optic pathway ganglioma: case study. *Neuro Oncol*. 2006;8:79–82.
2. Ambros IM, Attarbaschi A, Rumpler S, et al. Neuroblastoma cells provoke Schwann cell proliferation in vitro. *Med Pediatr Oncol*. 2001;36:163–168.
3. Ballas K, Kontoulis TM, Papavasiliou A, et al. A rare case of malignant triton tumor with pluridirectional differentiation. *South Med J*. 2009;102:435–437.
4. Beschorner R, Mittelbronn M, Koerbel A, et al. Atypical teratoid-rhabdoid tumor spreading along the trigeminal nerve. *Pediatr Neurosurg*. 2006;42:258–263.
5. Biegel JA. Molecular genetics of atypical teratoid/rhabdoid tumor. *Neurosurg Focus*. 2006;20:E11.
6. Biegel JA, Zhou JY, Rorke LB, et al. Germ-line and acquired mutations of INI1 in atypical teratoid and rhabdoid tumors. *Cancer Res*. 1999;59:74–79.
7. Bourdeaut F, Fréneaux P, Thuille B, et al. hSNF5/INI1-deficient tumours and rhabdoid tumours are convergent but not fully overlapping entities. *J Pathol*. 2007;211:323–330.
8. Bourdeaut F, Ribeiro A, Paris R, et al. In neuroblastic tumours, Schwann cells do not harbour the genetic alterations of neuroblasts but may nevertheless share the same clonal origin. *Oncogene*. 2008;27:3066–3071.
9. Boyd C, Smith MJ, Kluwe L, et al. Alterations in the SMARCB1 (INI1) tumor suppressor gene in familial schwannomatosis. *Clin Genet*. 2008;74:358–366.
10. Cai G, Zhu X, Xu Y, et al. Case report of extrarenal rhabdoid tumor of pelvic retroperitoneum molecular profile of angiogenesis and its implication in new treatment strategy. *Cancer Biol Ther*. 2009;8:417–421.
11. Carter JM, O'Hara C, Dundas G, et al. Epithelioid malignant peripheral nerve sheath tumor arising in a schwannoma, in a patient with "neuroblastoma-like" schwannomatosis and a novel germline SMARCB1 mutation. *Am J Surg Pathol*. 2012;36:154–160.
12. Chacko G, Chacko AG, Dunham CP, et al. Atypical teratoid/rhabdoid tumor arising in the setting of a pleomorphic xanthoastrocytoma. *J Neurooncol*. 2007;84:217–222.
13. Cheng JX, Tretiakova M, Gong C, et al. Renal medullary carcinoma: rhabdoid features and the absence of INI1 expression as markers of aggressive behavior. *Mod Pathol*. 2008;21:647–652.
14. Christiaans I, Kenter SB, Brink HC, et al. Germline SMARCB1 mutation and somatic NF2 mutations in familial multiple meningiomas. *J Med Genet*. 2011;48:93–97.
15. Clark HB, Minesky JJ, Agrawal D, et al. Myelin basic protein and P2 protein are not immunohistochemical markers for Schwann cell neoplasms. A comparative study using antisera to S-100, P2, and myelin basic proteins. *Am J Pathol*. 1985;121:96–101.
16. Eaton KW, Tooke LS, Wainwright LM, et al. Spectrum of SMARCB1/INI1 mutations in familial and sporadic rhabdoid tumors. *Pediatr Blood Cancer*. 2011;56:7–15.
17. El Kababri M, André N, Carole C, et al. Atypical teratoid rhabdoid tumor in a child with neurofibromatosis 1. *Pediatr Blood Cancer*. 2006;46:267–268.
18. Garcés-Iñigo EF, Leung R, Sebire NJ, et al. Extrarenal rhabdoid tumours outside the central nervous system in infancy. *Pediatr Radiol*. 2009;39:817–822.
19. Gottfried ON, Viskochil DH, Couldwell WT. Neurofibromatosis type 1 and tumorigenesis: molecular mechanisms and therapeutic implications. *Neurosurg Focus*. 2010;28:E8.
20. Hadfield KD, Newman WG, Bowers NL, et al. Molecular characterisation of SMARCB1 and NF2 in familial and sporadic schwannomatosis. *J Med Genet*. 2008;45:332–339.
21. Hadfield KD, Smith MJ, Urquhart JE, et al. Rates of loss of heterozygosity and mitotic recombination in NF2 schwannomas, sporadic vestibular schwannomas and schwannomatosis schwannomas. *Oncogene*. 2010;29:6216–6221.
22. Hasselblatt M, Oyen F, Gesk S, et al. Cribriform neuroepithelial tumor (CRINET): a nonrhabdoid ventricular tumor with INI1 loss and relatively favorable prognosis. *J Neuropathol Exp Neurol*. 2009;68:1249–1255.
23. Hollmann TJ, Hornick JL. INI1-deficient tumors: diagnostic features and molecular genetics. *Am J Surg Pathol*. 2011;35:e47–e63.
24. Hornick JL, Dal Cin P, Fletcher CD. Loss of INI1 expression is characteristic of both conventional and proximal-type epithelioid sarcoma. *Am J Surg Pathol*. 2009;33:542–550.
25. Hulsebos TJ, Kenter SB, Jakobs ME, et al. SMARCB1/INI1 maternal germ line mosaicism in schwannomatosis. *Clin Genet*. 2010;77:86–91.
26. Hulsebos TJ, Plomp AS, Wolterman RA, et al. Germline mutation of INI1/SMARCB1 in familial schwannomatosis. *Am J Hum Genet*. 2007;80:805–810.
27. Judkins AR. Immunohistochemistry of INI1 expression: a new tool for old challenges in CNS and soft tissue pathology. *Adv Anat Pathol*. 2007;14:335–339.
28. Judkins AR, Mauger J, Ht A, et al. Immunohistochemical analysis of hSNF5/INI1 in pediatric CNS neoplasms. *Am J Surg Pathol*. 2004;28:644–650.
29. Kleinschmidt-DeMasters BK, Lovell MA, Donson AM, et al. Molecular array analyses of 51 pediatric tumors shows overlap between malignant intracranial ectomesenchymoma and MPNST but not medulloblastoma or atypical teratoid rhabdoid tumor. *Acta Neuropathol*. 2007;113:695–703.
30. Kohashi K, Oda Y, Yamamoto H, et al. SMARCB1/INI1 protein expression in round cell soft tissue sarcomas associated with chromosomal translocations involving EWS: a special reference to SMARCB1/INI1 negative variant extraskeletal myxoid chondrosarcoma. *Am J Surg Pathol*. 2008;32:1168–1174.
31. Kreiger PA, Judkins AR, Russo PA, et al. Loss of INI1 expression defines a unique subset of pediatric undifferentiated soft tissue sarcomas. *Mod Pathol*. 2009;22:142–150.
32. Kurtkaya-Yapicier O, Scheithauer BW, Woodruff JM, et al. Schwannoma with rhabdomyoblastic differentiation: a unique variant of malignant triton tumor. *Am J Surg Pathol*. 2003;27:848–853.
33. Oda Y, Tsuneyoshi M. Extrarenal rhabdoid tumors of soft tissue: clinicopathological and molecular genetic review and distinction from other soft-tissue sarcomas with rhabdoid features. *Pathol Int*. 2006;56:287–295.
34. Parwani AV, Herawi M, Volmar K, et al. Urothelial carcinoma with rhabdoid features: report of 6 cases. *Hum Pathol*. 2006;37:168–172.

35. Patil S, Perry A, Maccollin M, et al. Immunohistochemical analysis supports a role for INI1/SMARCB1 in hereditary forms of schwannomas, but not in solitary, sporadic schwannomas. *Brain Pathol*. 2008;18:517–519.
36. Roberts CW, Biegel JA. The role of SMARCB1/INI1 in development of rhabdoid tumor. *Cancer Biol Ther*. 2009;8:412–416.
37. Rousseau G, Noguchi T. Bourdon V, et al. SMARCB1/INI1 germline mutations contribute to 10% of sporadic schwannomatosis. *BMC Neurol*. 2011;11:9.
38. Russo P, Biegel JA. SMARCB1/INI1 alterations and hepatoblastoma: another extrarenal rhabdoid tumor revealed? *Pediatr Blood Cancer*. 2009;52:312–313.
39. Sestini R, Bacci C, Provenzano A, et al. Evidence of a four-hit mechanism involving SMARCB1 and NF2 in schwannomatosis-associated schwannomas. *Hum Mutat*. 2008;29:227–231.
40. Strom T, Kleinschmidt-Demasters BK, Donson A, et al. Rare nerve lesions of non- nerve sheath origin: a 17-year retrospective series. *Arch Pathol Lab Med*. 2009;133:1391–1402.
41. Swensen JJ, Keyser J, Coffin CM, et al. Familial occurrence of schwannomas and malignant rhabdoid tumour associated with a duplication in SMARCB1. *J Med Genet*. 2009;46:68–72.
42. Tuefferd M, De Bondt A, Van Den Wyngaert I, et al. Genome-wide copy number alterations detection in fresh frozen and matched FFPE samples using SNP 6.0 arrays. *Genes Chromosomes Cancer*. 2008;47:957–964.
43. Upadhyaya M. Genetic basis of tumorigenesis in NF1 malignant peripheral nerve sheath tumors. *Front Biosci*. 2011;16:937–951.
44. van den Munckhof P, Christiaans I, Kenter SB, et al. Germline SMARCB1 mutation predisposes to multiple meningiomas and schwannomas with preferential location of cranial meningiomas at the falx cerebri. *Neurogenetics*. 2012;13:1–7.
45. Versteege I, Sévenet N, Lange J, et al. Truncating mutations of hSNF5/INI1 in aggressive paediatric cancer. *Nature*. 1998;394:203–206.
46. Wykoff CC, Lam BL, Brathwaite CD, et al. Atypical teratoid/rhabdoid tumor arising from the third cranial nerve. *J Neuroophthalmol*. 2008;28:207–211.